Numerical study of physical properties of resistive wall modes in tokamaks*

Xia Xin-Nian(夏新念), Liu Yue(刘 悦)†, Liu Chao(刘 超), He Yu-Ling(何玉玲), and Xia Guo-Liang(夏国良)

Key Laboratory of Materials Modification by Laser, Ion and Electron Beams (Dalian University of Technology) Ministry of Education, School of Physics and Optoelectronic Engineering, Dalian University of Technology, Dalian 116024, *China*

(Received 30 March 2012; revised manuscript received 31 August 2012)

The effect of plasma with toroidal rotation on the resistive wall modes in tokamaks is studied numerically. An eigenvalue method is adopted to calculate the growth rate of the modes for changing plasma resistivity and plasma density distribution, as well as the diffusion time of magnetic field through the resistive wall. It is found that the resistive wall mode can be suppressed by the toroidal rotation of the plasma. Also, the growth rate of the resistive wall mode decreases when the edge plasma density is the same as the core plasma density, but it only changes slightly with the plasma resistivity.

Keywords: tokamak, resistive wall mode, toroidal rotation, plasma density distribution

PACS: 52.55.Fa, 52.55.Tn, 52.35.Py **DOI:** 10.1088/1674-1056/22/5/055203

1. Introduction

A high β value is required for plasmas with long-time steady operation in advanced tokamaks. While the external kink mode, as a macroscopic magnetohydrodynamic (MHD) instability, is one of the major obstacles that limits the high β value[1] in plasmas and can even cause termination of the discharge in tokamaks. It is found that the external kink mode can be stabilized by a perfectly conducting wall around the plasma that is close enough to the plasma.[2] Because of the finite resistivity of the external conducting wall, a new unstable mode (called resistive wall mode) appears near the wall,[3] and the resistive wall mode, driven by pressure or current, grows more slowly than the external kink mode, with an exponential growth time on the order of the diffusion time of the magnetic field through the wall ($\tau_{\rm w}$). In 1994, Bondeson and Ward were the first to find that the resistive wall mode can be stabilized when the plasma rotates at some fraction of the speed of sound. The stabilization depends on toroidal coupling to sound waves and is affected by ion Landau damping.[4,5] In 1995, Chu *et al.*[6] proved that plasma rotation with dissipation can fully stabilize the resistive wall mode at a critical rotation frequency. Further studies of the resistive wall mode shown that toroidal plasma rotation[7–9] and a feedback coil[10–12] around the resistive wall are both effective ways to stabilize the unstable mode. Subsequently, researchers found that the poloidal plasma rotation and plasma density[13] also affect the resistive wall mode. However, in 2007, an experimental study of Reimerdes *et al.*,[14] showed that the critical rotation frequency is about 0.3% of the Alfvén speed, much lower than the theoretical prediction. Recently, Li and Liu[15] calculated the dispersion relation of the resistive wall mode in a simplified slab model. They found that the resistive wall instability driven by plasma flow could be excited when the flow exceeded the critical velocity, but it could be stabilized when the flow increased sufficiently. However, the stability mechanism that would explain these experimental results is not clear. Recently, the effect of surface current on the resistive wall mode was studied by Cui *et al.*,[16] finding that for the equilibrium surface current profiles with δ-function, the plasma is stable and the plasma flow has little effect. For the step-function surface current, the system becomes stable more easily when the surface current layer is thicker, and the plasma flow still almost has no effect on the system. Relevant research on the effect of equilibrium current similar to the bootstrap current on MHD instabilities was reported by Li *et al.*[17] The narrower and higher the bump current profile is, the more stable the system is, and when the center of the current bump is close enough to the plasma surface, the plasma pressure becomes high. Also, many papers focused on the stabilization of the resistive wall mode by energetic particles.[18] The trapped energetic particles can stabilize the resistive wall mode when a resonance exists between the mode and the magnetic precession drift motion of energetic particles. And when the β of energetic particles exceeds a critical value, a fishbonelike bursting mode appears,[19] and this instability mode grows rapidly. Recently, it was found that the multiple critical values of β can cause the fishbonelike bursting mode.[20] In the present work, the effects of some physical parameters of plasma on the resistive wall mode are numerically studied

*Project supported by the National Natural Science Foundation of China (Grant Nos. 11275041, 11105065, 11095015, and 10675029) and the National Basic Research Program of China (Grant Nos. 2008CB717801, 2008CB787103, 2009GB105004, and 2010GB106002).

†Corresponding author. E-mail: liuyue@dlut.edu.cn

© 2013 Chinese Physical Society and IOP Publishing Ltd

to explore the difference of the critical rotation frequency between the experimental results and the theoretical results.

In 1992, Bondeson *et al.*[21] first created MARS code to research plasma instabilities, and then Chu *et al.* improved the code, considering the influence of non-uniform plasma rotation,[6] the control of feedback coil,[11] and the kinetic effects[22] in the code. MHD instabilities in plasmas always appear in the case of low mode,[23] so in this work, the growth rate of the unstable mode with poloidal mode number $m = 2$ and toroidal mode number $n = 1$ is studied.

In this work, the MARS code is adopted to investigate the instability of the resistive wall mode with toroidal plasma rotation. The main structure of this paper is as follows. In Section 2, a model, i.e., MHD equations, is given for research. Then, linearizing the equations, we obtain the eigenvalue equation of complex growth rate. Section 3 gives the results of the growth rate and real frequency of unstable mode varying with diffusion time, resistivity and density distribution of plasmas, and also a relevant explanation is given. Finally, a simple summary and a conclusion are given in Section 4.

2. Model

For the equilibrium, the plasma in tokamaks can be regarded as an ideal fluid. The ideal MHD equations are adopted for the equilibrium. In this work, the current profile in equilibrium is chosen with $J = J_0\left(1 - s^2/a^2\right)$, which is the same as that in the book[23] writen by Wesson. Here, a is the minor radius. In axisymmetric plasma, the magnetic field can be represented as $\boldsymbol{B} = F\nabla\phi + \nabla\phi \times \nabla\psi$, where F is the poloidal current flux function, ϕ is the toroidal angle, and ψ is the poloidal magnetic flux function. The pressure p and the poloidal current flux function F are functions of only ψ. Thus, an elliptic second-order partial differential equation, i.e., the Grad–Shafranov equation, $\nabla \cdot (\nabla\psi/R^2) = -p'(\psi) - FF'(\psi)/R^2$, is obtained, where R is the major radius.

The flux coordinate system of (s, χ, ϕ) is adopted, where the radial coordinate s is defined as a function of ψ, and χ is the poloidal angle. Using the finite element method to solve the Grad-Shafranov equation, the equilibrium profiles are given as functions of s. The equilibrium solution is the prerequisite for the MHD stability code MARS.

The MARS code adopts fluid simulation to study MHD instability. In this work, the drift motion of plasma particles is negligible, regarding that the pressure is a scalar. In order to study the stability of plasma, considering the plasma deviates from the equilibrium state, the growth rate of perturbed quantities is calculated. The resistive MHD equations are selected for the perturbed equations

$$\frac{\mathrm{d}\rho}{\mathrm{d}t} + \rho\nabla\cdot\boldsymbol{v} = 0, \tag{1}$$

$$\frac{\mathrm{d}p}{\mathrm{d}t} + \Gamma p\nabla\cdot\boldsymbol{v} = 0, \tag{2}$$

$$\frac{\mathrm{d}\boldsymbol{B}}{\mathrm{d}t} = (\boldsymbol{B}\cdot\nabla)\boldsymbol{v} - (\nabla\cdot\boldsymbol{v})\boldsymbol{B} - \nabla\times(\eta\boldsymbol{J}), \tag{3}$$

$$\rho\frac{\mathrm{d}\boldsymbol{v}}{\mathrm{d}t} = -\nabla p + \boldsymbol{J}\times\boldsymbol{B}, \tag{4}$$

where

$$\frac{\mathrm{d}}{\mathrm{d}t} = \frac{\partial}{\partial t} + \boldsymbol{v}\cdot\nabla. \tag{5}$$

Through linearizing and nondimensionalizing resistive MHD equations, with perturbed variables using a Fourier transform in the toroidal direction, the perturbed equations of plasma are obtained as follows:

$$(\gamma + \mathrm{i}n\Omega_0)\boldsymbol{\xi} = \boldsymbol{v}_1 + (\boldsymbol{\xi}\cdot\nabla\Omega_0)R^2\nabla\phi, \tag{6}$$

$$\rho_0(\gamma + \mathrm{i}n\Omega_0)\boldsymbol{v}_1 = -\nabla p_1 + \boldsymbol{J}_1\times\boldsymbol{B}_0 + \boldsymbol{J}_0\times\boldsymbol{B}_1 - \rho_0\boldsymbol{U}(\boldsymbol{v}_1), \tag{7}$$

$$(\gamma + \mathrm{i}n\Omega_0)\boldsymbol{B}_1 = \nabla\times(\boldsymbol{v}_1\times\boldsymbol{B}_0 - \eta\boldsymbol{J}_1) + (\boldsymbol{B}_1\cdot\nabla\Omega_0)R^2\nabla\phi, \tag{8}$$

$$\boldsymbol{J}_1 = \nabla\times\boldsymbol{B}_1, \tag{9}$$

$$(\gamma + \mathrm{i}n\Omega_0)p_1 = -(\boldsymbol{v}_1\cdot\nabla)p_0 - \Gamma p_0\nabla\cdot\boldsymbol{v}_1, \tag{10}$$

$$(\gamma + \mathrm{i}n\Omega_0)\rho_1 = -(\boldsymbol{v}_1\cdot\nabla)\rho_0 - \rho_0\nabla\cdot\boldsymbol{v}_1. \tag{11}$$

For the above equations, $(\rho, \boldsymbol{\xi}, \boldsymbol{v}, \boldsymbol{B}, \boldsymbol{J}, p)$ are used to represent plasma density, perturbed displacement, velocity, magnetic field, current density, and pressure, respectively. Perturbed displacement is shown as $\partial\boldsymbol{\xi}/\partial t + (\boldsymbol{v}_0\cdot\nabla)\boldsymbol{\xi} = \boldsymbol{v}_1 + (\boldsymbol{\xi}\cdot\nabla)\boldsymbol{v}_0 R\nabla\phi$. In these equations, the subscript 0 is used to denote the equilibrium quantities, whereas the subscript 1 denotes the perturbed quantities, Ω_0 is the toroidal plasma rotation frequency when plasma is in the equilibrium state, and it is a function of only the flux function, γ is the complex growth rate of the unstable modes, Γ is the ratio of specific heats, η is the plasma resistivity. Compared with the ideal MHD equations, the fourth term in the right of Eq. (7) is the Coriolis force caused by the plasma velocity. The first term on the right of Eq. (8) represents the generalized Ohm's law, and the second is the Doppler shifts. It is seen that the density equation (Eq. (9)) is decoupled from other equations, therefore, it can be solved independently.

From these eigenvalue equations of the growth rate, the eigenvalue and the eigenfunction of the mode are calculated with the MARS code.

3. Result

Except for additional explanation in this paper, some parameters are as follows: the edge safety factor $q_\mathrm{a} = 1.75$, the diffusion time of resistive wall $\tau_\mathrm{w} = 3.0\times10^3\ \tau_\mathrm{A}$, plasma resistivity $\eta = 0$, the distribution of plasma density $\rho_1/\rho_0 = 1$, the wall position $b/a = 1.21$, the aspect ratio $a/R_0 = 0.1$, τ_A is the Alfvén time scale, and Ω_A is the Alfvén frequency.

3.1. Instabilities with different wall positions without plasma rotation

Figure 1 gives the growth rate of the modes in the cases of the plasmas surrounded by no wall, the resistive wall, and a perfectly conducting wall. In all three cases, the plasmas have no rotation, and $m = 2$, $n = 1$.

As in the previous research, both in theory and in experiment, at the range of the critical wall position, the external kink mode can be stabilized by a perfectly conducting wall. In this work, from our calculations, we find that the critical wall position b_c/a is about 1.25. For the resistive wall, when $b_c/a < 1.25$, the growth rate of the mode γ reduces with the resistive wall moving closer to the plasma, but it is always positive. This means that the unstable mode cannot be stabilized in this case.

Figure 2(a) gives the safety factor q profile with the edge safety factor $q_a = 1.75$, and figure 2(b) gives the growth rate of the external kink mode with the edge safety factor when $m = 2$ and $n = 1$. Note that when $m = 2$ and $n = 1$, the MHD instability almost appears in the range for edge safety factor $q_a = 1.47$–2.0, and the growth rate has its maximum value at about $q_a = 1.7$. Figure 2(c) gives the growth rate with the edge safety factor in the case of a resistive wall, where the flux diffusion time of resistive wall is $\tau_w = 3.0 \times 10^3\ \tau_A$. It is found that the growth rate of the mode with the plasma surrounded by the resistive wall is smaller than that of the external kink mode. When the resistive wall moves close enough to the plasma, the growth rate becomes lower, but it is always positive. Therefore, the unstable mode cannot be stabilized in the case of existing resistivity in the external conducting wall.

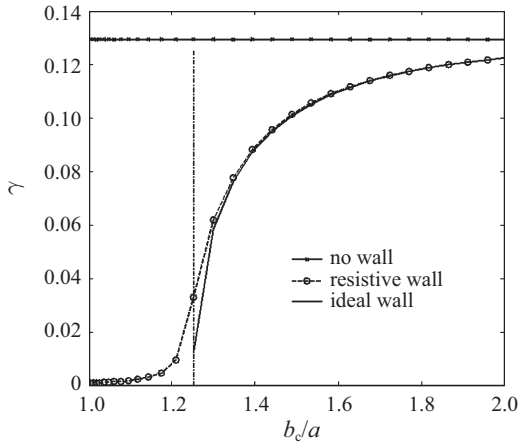


Fig. 1. Growth rate γ versus the wall position b_c/a.

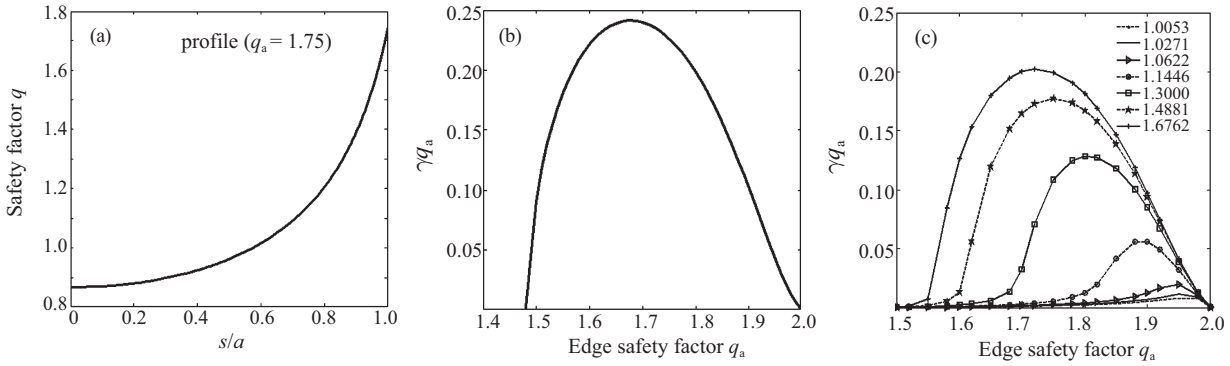


Fig. 2. (a) Profile of the safety factor. (b) The growth rate of the external kink mode versus the edge safety factor. (c) The growth rate versus the edge safety factor in the cases: $b/a = 1.0053$, 1.0271, 1.0622, 1.1446, 1.3, 1.4881, and 1.6762, respectively.

3.2. Resistive wall mode with toroidal plasma rotation

As shown in Fig. 3, the growth rate of the mode changes with the wall position. Here, diffusion time of the wall is $\tau_w = 3.0 \times 10^3\ \tau_A$ and the edge safety factor is $q_a = 1.75$. The unstable mode is separated into two parts. One is wall mode, in which the unstable mode locked on the wall changes significantly with the increase of the plasma rotation. The other is plasma mode, in which the unstable mode which has a slow response to plasma rotation is locked on the plasma. As seen in the figure, when the rotation frequency increases initially, the growth rate increases a little, when the plasma rotation continues to increase, the growth rate reduces. Note that as the plasma rotation increases, the growth rate of the unstable mode changes significantly when the wall position b/a ranges from 1.14 to 1.22, and when the rotation frequency gets larger, the curves in this region decline dramatically. When the wall position is near $b/a = 1.35$, the growth rate hardly changes with the plasma rotation. As dissipation is not considered here, a stability window cannot be seen. The growth is nearly zero with a large plasma rotation, but never reaches zero or becomes negative without any dissipation. The results are in accordance with the description in Ref. [6].

As known from Fig. 3, for wall position $b/a < 1.25$, because of the great effect of plasma rotation on the growth rate of the mode, the dependence of the growth rate on the plasma rotation with different parameters is investigated. In Fig. 4(a), the growth rate changes with toroidal rotation frequency is shown. In Fig. 4(b), the curves represent the cor-

responding real frequencies of the unstable modes. It can be seen that the growth rate increases with the plasma rotation initially, but when the rotation frequency exceeds a certain value, the growth rate becomes smaller. When the wall position $b/a = 1.1189$, the wall is close to the plasma, and the unstable mode is locked on the wall. The real frequency is small compared with the rotation frequency. When the wall is a bit far from the plasma ($b/a = 1.21$), the effect of the wall on the plasma becomes weak, and the real frequency of the mode grows faster.

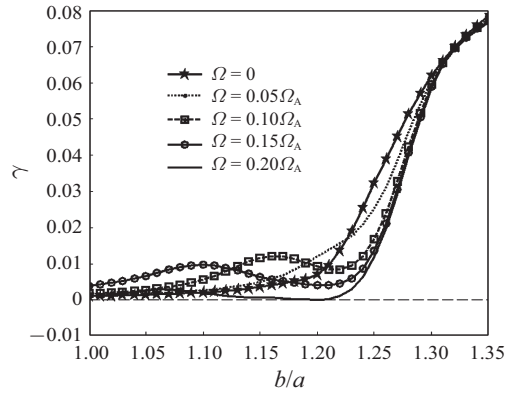


Fig. 3. The growth rate versus the position of wall with different rotation frequencies, the toroidal rotation frequencies are $\Omega = 0.0$, $0.05\Omega_A$, $0.10\Omega_A$, $0.15\Omega_A$, and $0.20\Omega_A$, respectively.

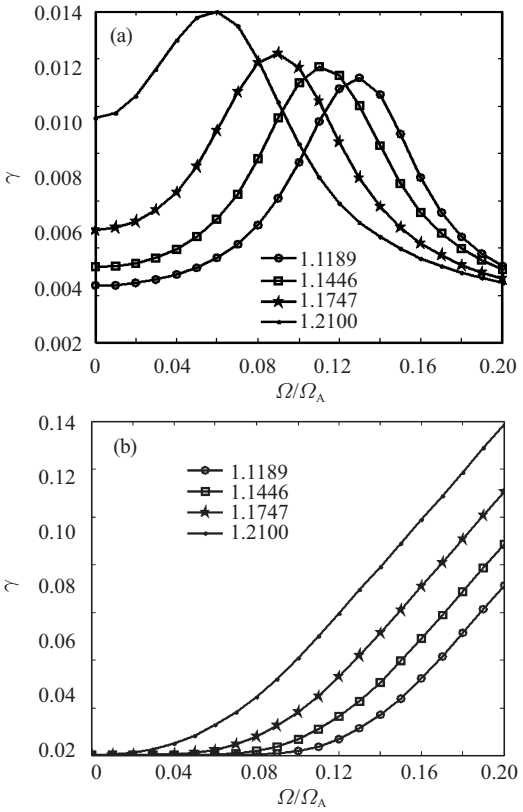


Fig. 4. Dependence of (a) linear growth rate and (b) real frequency on the rotation frequency with different positions of wall $b/a = 1.1189$, 1.1446, 1.1747, and 1.21, respectively.

3.3. Instabilities with magnetic field diffusion time through the wall

Figures 5(a) and 5(b) are the growth rate and the real frequency of the mode changing with toroidal plasma rotation, separately. Here, the wall position is $b/a = 1.21$. As seen from the figure, the growth rate is slower with long diffusion time of the wall. If the diffusion time is long enough, i.e., the resistive wall is very nearly an ideal wall, so the unstable mode can be stabilized. Since the diffusion time is long, the magnetic field which restrains plasmas will slowly permeate the wall. Therefore, the growth rate gets smaller. While the diffusion time tends to zero, plasmas seem to be at a free boundary condition, and the growth rate is very large.

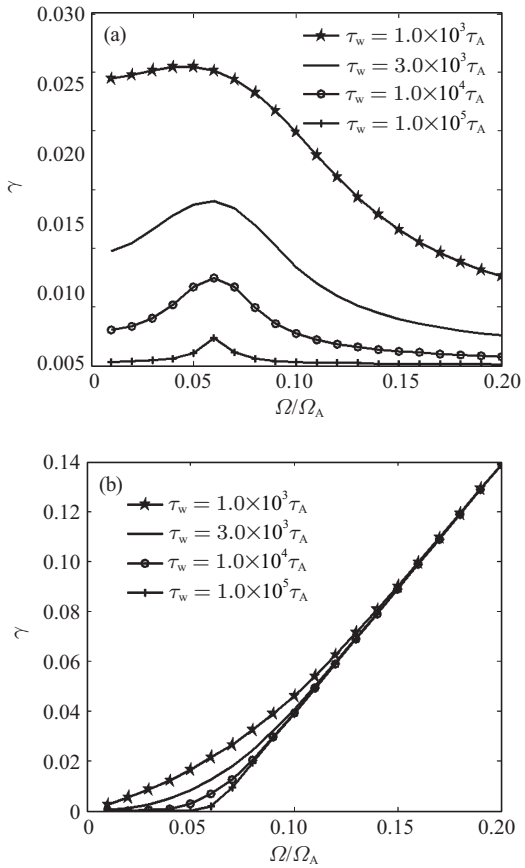


Fig. 5. Dependence of (a) growth rate γ and (b) real frequency ω_r on rotation frequency Ω/Ω_A with different diffusion time, the diffusion time are $\tau_w = 1.0 \times 10^3 \tau_A$, $3.0 \times 10^3 \tau_A$, $1.0 \times 10^4 \tau_A$, and $1.0 \times 10^5 \tau_A$, respectively.

The relationship between the growth rate of the resistive wall mode and the diffusion time is best seen in Fig. 6. In Fig. 6(b), the ordinate axis shows the product of diffusion time and the growth rate. Note that as the diffusion time becomes longer, the curves turn into straight lines parallel to the horizontal axis. This indicates that the product tends to be a fixed value for large enough diffusion time.

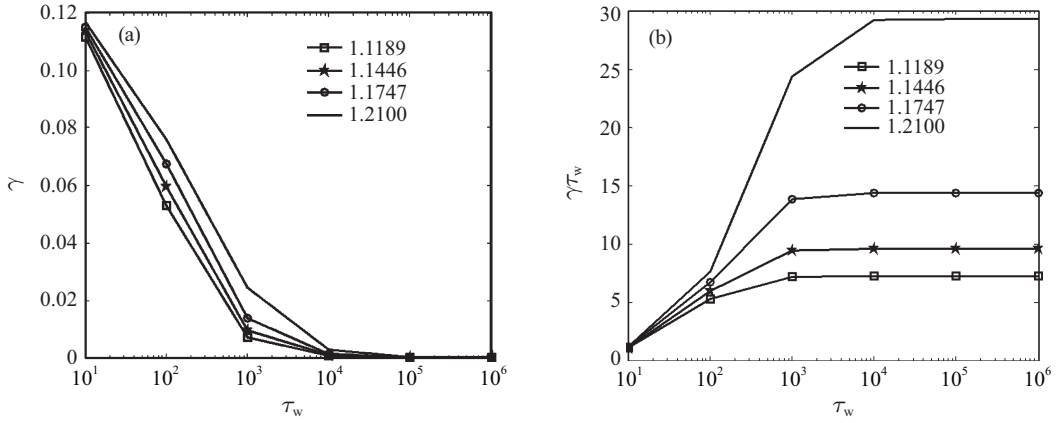


Fig. 6. The relation between (a) the growth rate γ and (b) the diffusion time τ_w with different positions of wall. The wall positions are $b/a = 1.1189$, 1.1446, 1.1747, and 1.21, respectively.

3.4. Instabilities with plasma resistivity

The growth rate and real frequency of the resistive wall mode changes versus plasma resistivity with wall position $b/a = 1.21$ are shown in Fig. 7. It can be seen that growth rate changes slightly with changing plasma resistivity, while the real frequency hardly changes.

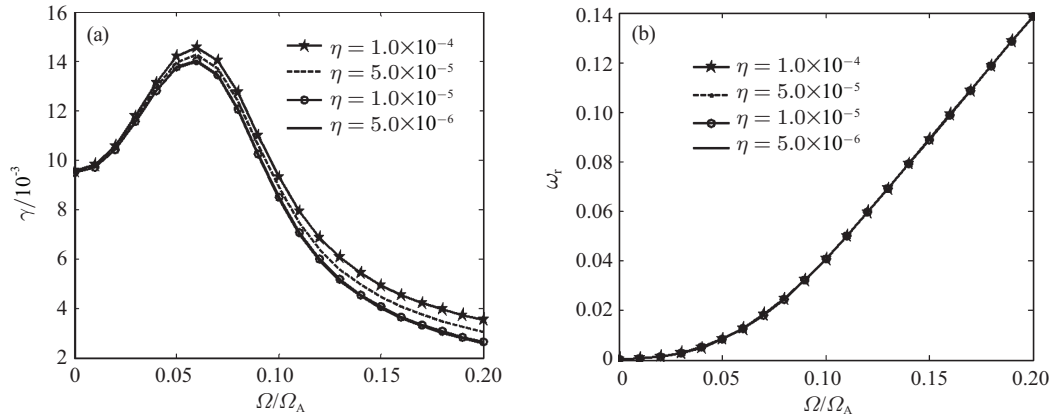


Fig. 7. Dependence of (a) growth rate γ and (b) real frequency ω_r on the rotation frequency with different plasma resistivity. The plasma resistivities are $\eta = 1.0 \times 10^{-4}$, 5.0×10^{-5}, 1.0×10^{-5}, and 5.0×10^{-6}, respectively.

3.5. Instabilities with different plasma density distributions

The profile of the plasma density distribution is shown in Fig. 8(a). The curve with the asterisk is the distribution of $\rho_e/\rho_c = 1$, which represents the plasma distributed uniformly in space. Here, ρ_e indicates the edge density of the plasma, and ρ_c is the core density of the plasma. The changing growth rate and real frequency are shown in Figs. 8(b) and 8(c). It can be seen from the figures that the growth rate decreases when the edge plasma density gets as large as the core plasma density. But when $\rho_e/\rho_c = 1$, the real frequency is the largest.

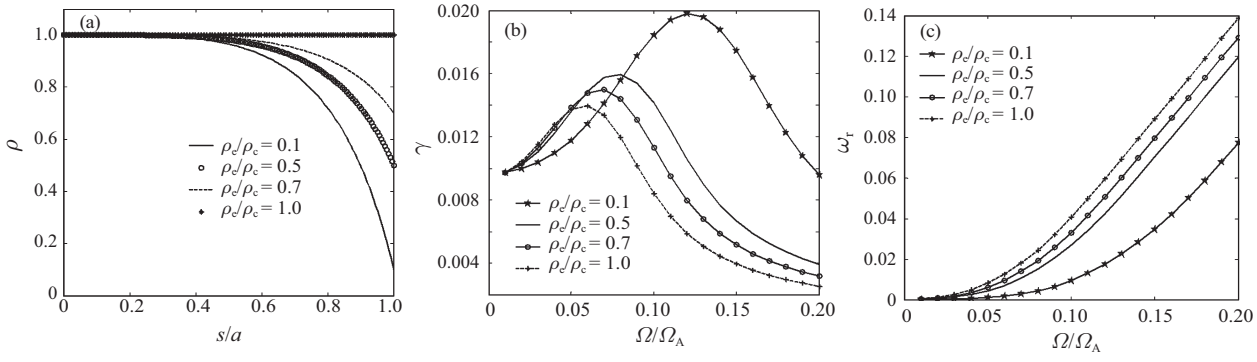


Fig. 8. (a) Plasma density distributions in four cases: $\rho_e/\rho_c = 0.1$, 0.5, 0.7 and 1. The dependence of (b) growth rate γ and (c) real frequency ω_τ on rotation frequency with different density distributions.

4. Conclusion

A study of the effect of the plasma parameters on the resistive wall mode with and without the plasma rotation was carried out. It is found that the plasma rotation can suppress the resistive wall mode when the wall is close to the plasma, whereas when the wall is far from the plasma, the plasma rotation has a weak effect on the unstable mode. Through changing some plasma parameters, conclusions are obtained as follows.

No matter whether the wall surrounding the plasma is an ideal wall or a resistive wall, as long as the wall is far from the plasma, the influence of the wall on the growth rate of the mode is weak. The growth rate of the mode is on the same order as that of the external kink mode. However when the wall is close enough to the plasma, the unstable mode is locked on the external conducting wall. At this moment, the real frequency of the mode changes slightly with the plasma rotation. The longer the diffusion time of the external conducting wall is, the smaller the growth rate of the mode is, because the resistive wall seems to be a perfectly conducting wall. For a large enough diffusion time, the growth rate changes inversely with the diffusion time, i.e., $\gamma \propto 1/\tau_{\rm w}$.

The plasma resistivity has a weak effect on the resistive wall mode. The change of the plasma density distribution makes a difference in both the growth rate and the real frequency of the resistive wall mode. The growth rate reduces with the higher edge plasma density. When the edge plasma has the same density as the core plasma the growth rate is lower. While the real frequency of the mode is on the opposite side, it reduces with lower edge density. Mechanisms for stabilizing the resistive wall mode are studied, but the viscosity is not considered in this work, and in future work, more factors will be considered for stabilizing the resistive wall mode.

References

[1] Strait E J 1994 *Phys. Plasmas* **1** 1415
[2] Gimblett C G 1986 *Nucl. Fusion* **26** 617
[3] Freidberg J P 1987 *Ideal Magnetohyhdrodynamics* (New York: Plenum Press) p. 481
[4] Bondeson A and Ward D J 1994 *Phys. Rev. Lett.* **72** 2709
[5] Ward D J and Bondeson A 1995 *Phys. Plasmas* **2** 1570
[6] Chu M S, Greene J M, Jensen T H, Miller R L, Bondeson A, Johnson R W and Mauel M E 1995 *Phys. Plasmas* **2** 2236
[7] Chu M S and Okabayashi M 2010 *Plasma Phys. Controlled Fusion* **52** 123001
[8] Betti R and Freidberg J P 1995 *Phys. Rev. Lett.* **74** 2949
[9] Cui S Y, Wang X G and Liu Y 2006 *Phys. Plasmas* **13** 094506
[10] Liu Y Q, Bondeson A, Fransson C M, Lennartson B and Breitholtz C 2000 *Phys. Plasmas* **7** 3681
[11] Fransson C M, Lennartson B, Breitholtz C, Bondeson A and Liu Y Q 2000 *Phys. Plasmas* **7** 4143
[12] Li L, Liu Y and Liu Y Q 2012 *Phys. Plasmas* **19** 012502
[13] Sato M and Nakajima N 2006 *Phys. Plasmas* **13** 102507
[14] Reimerdes H, Garofalo A M, Jackson G L, Okabayashi M, Strait E J, Chu M S, In Y, La Haye R J, Lanctot M J, Liu Y Q, Navratil G A, Solomon W M, Takahashi H and Groebner R J 2007 *Phys. Rev. Lett.* **98** 055001
[15] Li L and Liu Y 2012 *Chin. Phys. Lett.* **29** 075204
[16] Cui S Y, Lu G M and Liu Y 2012 *J. Plasma Phys.* **78** 501
[17] Li L, Liu Y, Xu X Y and Xia X N 2012 *Plasma Sci. Technol.* **14** 14
[18] Hao G Z, Liu Y Q, Wang A K, Jiang H B, Lu G, He H D and Qiu X M 2011 *Phys. Plasmas* **18** 032513
[19] Hao G Z, Wang A K, Liu Y Q and Qiu X M 2011 *Phys. Rev. Lett.* **107** 015001
[20] Hao G Z, Liu Y Q, Wang A K and Qiu X M 2012 *Phys. Plasmas* **19** 032507
[21] Bondeson A, Vlad G and Lutjens H 1992 *Phys. Fluids B* **4** 1889
[22] Liu Y Q, Chu M S, Chapman I T and Hender T C 2008 *Phys. Plasmas* **15** 112503
[23] Wesson J A 2004 *Tokamaks* (Oxford: Clarendon Press) p. 749